SCIENCE CHINA
Chemistry

• ARTICLES •

December 2010 Vol.53 No.12: 2657–2662
doi: 10.1007/s11426-010-4157-y

Heterogeneous reactions of gaseous methanesulfonic acid with calcium carbonate and kaolinite particles

TANG MingJin, LI MengQiu & ZHU Tong*

State Key Joint Laboratory of Environmental Simulation and Pollution Control; College of Environmental Sciences and Engineering, Peking University, Beijing 100871, China

Received July 2, 2010; accepted September 24, 2010

Heterogeneous reactions of gaseous methanesulfonic acid (MSA) with calcium carbonate ($CaCO_3$) and kaolinite particles at room temperature were investigated using diffuse reflectance infrared Fourier transform spectroscopy (DRIFTS) and ion chromatography (IC). Methanesulfonate (MS^-) was identified as the product in the condensed phase, in accordance with the product of the reaction of gaseous MSA with NaCl and sea salt particles. When the concentration of gaseous MSA was 1.34×10^{13} molecules cm^{-3}, the uptake coefficient was $(1.21\pm0.06)\times10^{-8}$ (1 σ) for the reaction of gaseous MSA with $CaCO_3$ and $(4.10\pm0.65)\times10^{-10}$ (1 σ) for the reaction with kaolinite. Both uptake coefficients were significantly smaller than those of the reactions of gaseous MSA with NaCl and sea salt particles.

gaseous MSA, heterogeneous reaction, calcium carbonate, kaolinite

1 Introduction

CLAW hypothesis suggests that dimethyl sulfide (DMS) plays an important role in climate change via radiative forcing of sulfate aerosols, which are formed through the oxidation of DMS after its emission into the atmosphere from the surface of oceans [1]. Once emitted into the atmosphere, DMS can be oxidized by a variety of oxidants, including OH, NO_3, O_3, Cl, and BrO, to form a number of products, such as sulfur dioxide (SO_2), dimethylsulfoxide (DMSO), dimethylsulfone ($DMSO_2$), methanesulfonic acid/methanesulfonate (MSA/MS^-), and sulfate [2]. Advances in the investigation of gas-phase reactions of DMS and its products with oxidants such as OH and NO_3 have helped to elucidate DMS oxidation mechanisms; however, increasing numbers of field and modeling studies suggest that gas-phase reactions alone cannot fully explain atmospheric DMS oxidation and the distribution of its oxidation products [2].

Gaseous MSA and MS^- are among the most important intermediate products of DMS oxidation in the marine and coastal boundary layer [3–5]. However, the gas-to-particle conversion of gaseous MSA alone cannot explain the observed levels of MS^- in aerosols [4, 5]. It was found that terrestrial ecosystems such as tropical rain forests and paddies may also emit DMS [6, 7]; more importantly, MS^- in aerosols was frequently detected in Beijing, China, where there is no obvious marine influence [8, 9].

Mineral dust aerosols, presently with an estimated emission rate of approximately 2000 Tg per year [10–12], is the second most abundant natural source of aerosols in the atmosphere [13]. After emitted into the atmosphere, they can be transported by several thousand kilometers [13, 14]. Their emission, long-range transportation, and deposition have a variety of impacts on biogeochemical cycles. For example, they can deposit various nutrients into the ocean and thus change marine primary production rates [15, 16]. In addition, they can influence the levels of many trace gases including OH, O_3, NO_x, and NO_y by heterogeneous reactions [17, 18]. Considering the important impact of

*Corresponding author (email: tzhu@pku.edu.cn)

mineral dust on many tropospheric chemical processes, it might also influence the scavenging of gaseous MSA and formation of MS^- in aerosols.

Several studies have investigated the mass accommodation of gaseous MSA on liquid surfaces. De Bruyn *et al.* [19] studied the mass accommodation of gaseous MSA on NaCl surface via a low-pressure reactor coupled with mass spectrometry, and found that the mass accommodation coefficient was independent of pH (1–14) and NaCl concentration (0–3.5 M), and negatively correlated with temperature (260–280 K). Schweitzer *et al.* [20] used the droplet train technique combined with mass spectrometry and Fourier transform infrared spectroscopy (FTIR) to study the mass accommodation of gaseous MSA on NaCl surface, and reported that the mass accommodation coefficient of gaseous MSA was independent of NaCl concentration (0–2 M), and it decreased from 0.16 to 0.1 when the temperature increased from 261 to 283 K. These two studies agree well. However, Hanson [21] reported a significantly larger mass accommodation coefficient, close to unity at 295–297.5 K, using a laminar flow reactor combined with chemical ionization mass spectrometry. More recently, Zhu *et al.* [22] investigated the heterogeneous reactions of gaseous MSA with NaCl and sea salt particles via diffuse reflectance infrared Fourier transform spectrometry (DRIFTS) and X-ray photoelectron spectroscopy (XPS), and reported a steady-state uptake coefficient of $(5.94 \pm 2.32) \times 10^{-7}$ (1 σ) for the reaction with NaCl and $(2.23 \pm 1.25) \times 10^{-7}$ (1 σ) for the reaction with sea salt. To the best of our knowledge, it is the only study to investigate the heterogeneous reaction of gaseous MSA with solid particles, and up to now there is no study on the heterogeneous reaction of gaseous MSA with mineral dust.

2 Experimental

2.1 Experimental apparatus

The experimental apparatus is described in detail in our previous study [22], here only key features are presented. It consisted of the gaseous MSA generation system and the reactor coupled with DRIFTS. Gaseous MSA was introduced into the DRIFTS system by passing N_2 (purity > 99.99%; Dept. of Mechanics and Engineering, Peking University) through a bubbler containing liquid MSA. It was confirmed in our previous study that gaseous MSA produced by this method was saturated [22]. The total flow rate of N_2 was regulated by the first mass flow controller (MFC1; 200 sccm) and the concentration of gaseous MSA in the reactor was regulated by adjusting the flow (via the second mass flow controller, MFC2) which passed through the liquid MSA bubbler. Due to the potentially strong adsorption of gaseous MSA on the surface, the inner walls of the reactor and the tubes were all coated with teflon and the tubing length was made as short as possible. In addition, the entire system was pre-equilibrated with gaseous MSA of the same concentration for 1 h before each experiment to saturate the surfaces of the reaction system.

The continuous flow apparatus consisted of a Nicolet Nexus FTIR spectrometer (Thermo Nicolet, Madison, WI, USA) equipped with a mercury cadmium telluride detector, a Harrick diffuse reflectance accessory (model DRA-2CS; Harrick Scientific, Hillsboro, OR, USA), and a stainless steel reactor with teflon-coated inner walls. Spectra were taken every 5 min with 128 scans in 2 min at 4 cm^{-1} resolution.

$CaCO_3$, with a stated purity of > 99.995%, CH_3SO_3Na, with a stated purity of > 98%, and liquid MSA, with a stated purity of > 99.5%, were supplied by Sigma-Aldrich (St. Louis, MO, USA). Kaolinite, with a stated purity of > 97%, was supplied by Shantou Xilong Chemicals (Shantou, China). $CaCO_3$ powders consisted of particles of several micrometers in size and were used without pretreatment, while larger kaolinite particles were ground in a mill for 30 min. Weighed samples of $CaCO_3$ (40 ± 5 mg) or pre-ground kaolinite (30 ± 3 mg) were packed into stainless steel sampling cups (9 mm × 0.5 mm), pressed evenly with a clean glass slide, and then placed into the reactor to react with gaseous MSA.

2.2 Characterization of particles

The volumetric Brunauer, Emmett, and Teller model (BET) surface area of $CaCO_3$ and kaolinite particles was measured with a BET apparatus (ASAP2010; Micromeritics Corporation, Norcross, GA, USA). The BET surface area of $CaCO_3$ particles was 0.8772 m^2/g, equivalent to the surface area of nonporous cubic particles with the size of 2.52 μm, and the BET surface area of kaolinite particles was 24.1059 m^2/g.

Scanning electron microscopy (SEM; Amray-1910FE; Amray Inc., San Jose, CA, USA) was used to observe the size and surface morphology of $CaCO_3$ and kaolinite particles. The diameters of most $CaCO_3$ and kaolinite particles (after ground in the mill) were in the range of several micrometers. The diameter of $CaCO_3$ observed by SEM was reasonably consistent with the diameter calculated from the BET surface area, indicating that $CaCO_3$ particles were nonporous, while the diameter of kaolinite observed by SEM was much larger than the diameter calculated from the BET surface area, suggesting that kaolinite particles are porous.

In addition, the elemental composition of kaolinite was analyzed by XPS (AXIS Ultra spectrometer; Kratos, Manchester, UK) with a focused monochromatized X-ray source (Al Kα) operated at 225 W with a corresponding voltage of 15 kV. The major elements in the particles were O, Si, and Al, in agreement with the available data [23]. The adsorbed organics on the kaolinite surface was below the detection limit of XPS.

2.3 Ion chromatography analysis

Ion chromatography (IC, Dionex DX-500) was used to measure MS^- concentration in the solution used to absorb gaseous MSA and MS^- concentration produced in condensed phase after the heterogeneous reactions. The IC instrument consisted of a Dionex Ionpac AS11 separation column, a Dionex Ionpac AS-14HC-4 mm guard column, a Dionex Ionpac ED50 self-regenerating suppressed conductivity detector, a Dionex Ionpac GP50 gradient pump, and a Dionex PeakNet 6.2 chromatographic workstation. To measure the gaseous MSA concentration, 10.00 mL deionized water was used to absorb gaseous MSA in N_2 carrier gas which passed through liquid MSA under 23 °C. Standard solutions with different concentrations of MS^- were prepared by dissolving weighted solid CH_3SO_3Na, and then were analyzed by IC to calibrate the measured MS^- concentration. The calibration curves are shown in Figure 1.

After the reaction with gaseous MSA for a controlled period of time, particles ($CaCO_3$ or kaolinite) along with the sampling cup were transferred to 10.00 mL deionized water, extracted for 15 min in an ultrasonic bath, filtered using a 0.45 μm micro-porous membrane (the diameter was 25 mm, Beijing Chemical Factory, China), and then analyzed by IC.

Empty sampling cups were kept in the reactor for the same time and exposed to gaseous MSA of the same concentration; after that, they were treated in the same way as the sampling cups with reacted particles, and then analyzed by IC. The MS^- concentration of these blanks was typically below the detection limit. Nevertheless, the concentrations of MS^- in the reacted samples were reported after the concentrations of corresponding blanks were subtracted.

Some MS^- might be strongly adsorbed by the particles (especially for kaolinite due to its large BET surface area) and could not be completely extracted into the solution via the method adopted here. Therefore, the amount of MS^- which was adsorbed by dust particles was measured using the followed method: particles with the same mass as the samples used in the reaction were added to the standard solutions with different concentrations of MS^-, and then they were extracted and analyzed in the same way. As shown in Figure 1, IC peak area of MS^- was 4% lower for $CaCO_3$-added solution and 8% lower for kaolinite-added solution than that of non-dust-added standard solution, indicating that MS^- produced on the $CaCO_3$ and kaolinite particles were only underestimated by 4% and 8% by this measurement, respectively.

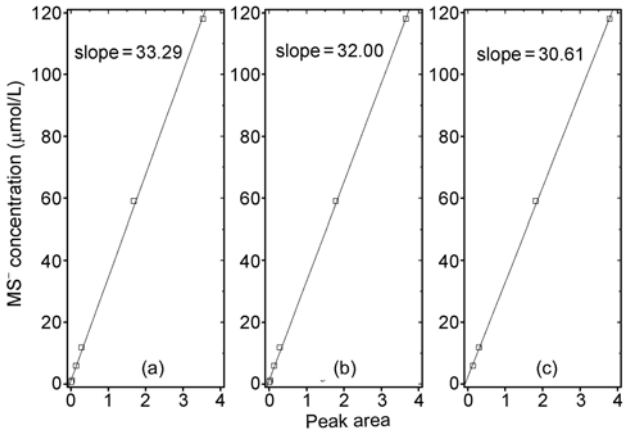

Figure 1 Calibration curves for MS^-. (a) MS^- standard solution; (b) $CaCO_3$-added MS^- standard solution; (c) kaolinite-added MS^- standard solution.

All of the solutions were analyzed by IC with the same method. The eluent, consisting of 10 mmol/L NaOH solution, was maintained at a flow rate of 1 mL/min for a total analysis time of 15 min. Under this condition, the retention time of MS^- was about 4.5 min for all the solutions.

3 Results and discussion

3.1 Reaction products

The IR spectra taken during the reaction of $CaCO_3$ particles with gaseous MSA showed three major absorption bands: ~790 cm^{-1}, out-of-plane bend of S=O bond; ~1090 cm^{-1}, symmetric stretch of S=O bond; and ~ 1220 cm^{-1}, antisymmetric stretch of S=O bond. The IR spectra of $CaCO_3$ particles after the reaction with gaseous MSA were in good agreement with the spectrum of the mixture of CH_3SO_3Na in NaCl, as shown in Figure 2.

In addition, a peak at about 1160 cm^{-1} appeared in the spectrum of reacted particles, perhaps due to the split of the major peak at 1220 cm^{-1}. The peak at 1090 cm^{-1} was slightly shifted compared to the spectrum of the CH_3SO_3Na/NaCl mixture, and it shifted towards higher wavenumbers as the reaction processed. These phenomena indicated the change in the microenvironments of the MS^- ions formed on $CaCO_3$ particles: during the reaction of $CaCO_3$ with gaseous MSA, crystalline MS^- ions, small amounts of isolated MS^-, and adsorbed MSA were formed; however, only CH_3SO_3Na crystals existed in the CH_3SO_3Na/NaCl mixture. Similar splits and shifts of peaks in the spectra were also reported in our previous study on heterogeneous reactions of gaseous MSA with NaCl and sea salt particles [22]. Using DRIFTS to study the reaction of NO_2 with NaCl, Vogt and Finlayson-Pitts [24] found that the spectra of the product (NO_3^-) changed slightly during the reaction due to a gradual change of the formed NO_3^- from isolated ions to crystals.

After the reaction, $CaCO_3$ and kaolinite particles were analyzed by IC as described before. Except for a peak with a retention time of about 4.5 min, which corresponded to MS^-, no other obvious peaks appeared in the chromatograms. They were in agreement with the results of $CaCO_3$-added and kaolinite-added MS^- standard solution, suggesting that MS^- or surface-adsorbed MSA were formed

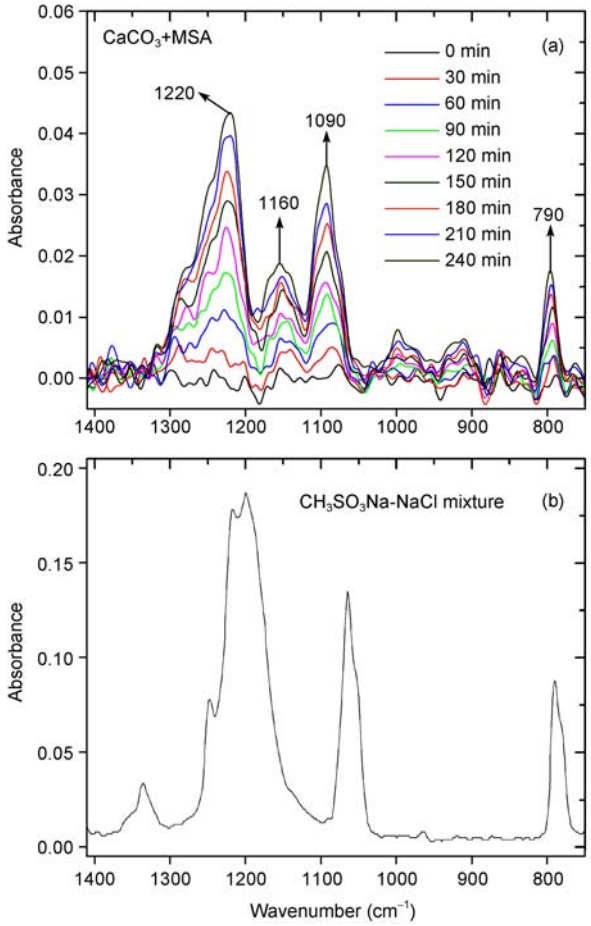

Figure 2 (a) IR spectra of the $CaCO_3$ particles as the function of the reaction time with gaseous MSA. The concentration of gaseous MSA was 1.34×10^{13} molecules/cm^3; (b) IR spectrum of the mixture of CH_3SO_3Na/NaCl.

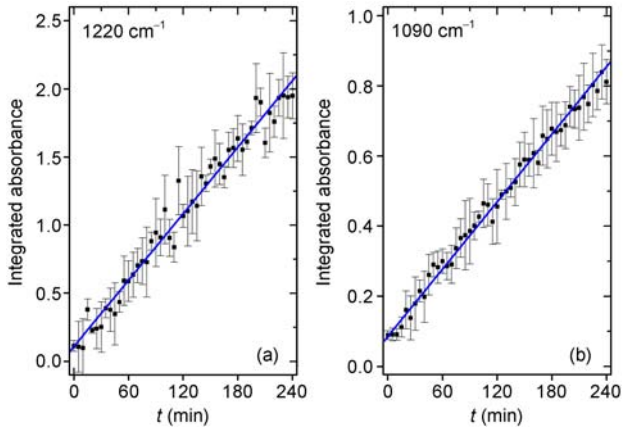

Figure 3 Integrated absorbance of two IR peaks of the products of the reaction of $CaCO_3$ with gaseous MSA, as the function of reaction time. (a) Integrated absorbance at 1220 cm^{-1}; (b) integrated absorbance at 1090 cm^{-1}.

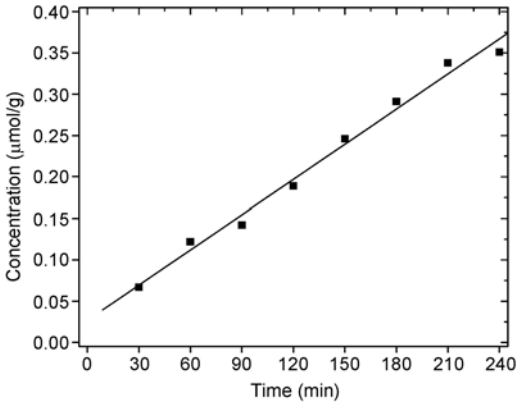

Figure 4 Bulk concentration of MS^- (measured by IC) formed in the condensed phase for the reaction of $CaCO_3$ particles with gaseous MSA, as a function of reaction time.

in the reaction of $CaCO_3$ and kaolinite particles with gaseous MSA.

3.2 Methanesulfonate production rates

Figure 3 shows the integrated absorbance of two IR peaks of $CaCO_3$ particles as the function of reaction time with gaseous MSA. Both increased linearly with reaction time, which confirms further that the peaks at 1220 and 1090 cm^{-1} were attributable to the formation of MS^- on the particles. In addition, the concentration of MS^- formed in the bulk particles also increased linearly with reaction time, as shown in Figure 4. In the study of heterogeneous reactions, DRIFTS is widely used to measure the surface concentration of the products while IC is used to analyze the bulk concentration. Li *et al.* [25] found that the bulk concentration of nitrate formed in the heterogeneous reaction of NaCl with NO_2 increased linearly, while the production rate of the nitrate on the surface decreased with reaction time.

The reaction of gaseous species with bulk particles first occurred mainly on the particles of the top layer(s), then on these of underlying layers. The sampling cups used by Li *et al.* [25] and also in this study were all 0.5 mm in depth. DRIFTS can only detect concentrations of compounds to depths of several micrometers, while IC measures the bulk concentration. This difference, according to Li *et al.* [25], led to the different increasing trends of the nitrate concentration measured by DRIFT and IC. However, in the present study, the MS^- concentrations detected by DRIFTS and IC both increased linearly with reaction time; this may indicate that the reaction rates of gaseous MSA with $CaCO_3$ were the same in the top layers and in the underlying layers, or that the reaction was limited to the top layers within the detection depth of DRIFTS. We are inclined to the latter explanation, though more studies should be conducted to clarify this issue.

3.3 Possible mechanisms

It is widely believed that due to the hydrolysis of adsorbed

water on the surface:

$$CaCO_{3(s)} + H_2O_{(ad)} \rightarrow Ca(OH)(CO_3H)_{(ad)} \quad (1)$$

OH groups exist on the surface of $CaCO_3$ and they cannot be eliminated even under vacuum conditions [26]. Al-Hosney and Grassian [26] suggested that in the reaction of gaseous acid with $CaCO_3$ particles, adsorbed H_2CO_3 was first formed on the surface and then decomposed to CO_2 and H_2O. According to this hypothesis, we suggest that the heterogeneous reaction of gaseous MSA with $CaCO_3$ consists of several elementary steps (reaction (2)–(4)), which include reaction (1) as the first step:

$$Ca(OH)(CO_3H)_{(ad)} + CH_3SO_3H_{(g)} \rightarrow Ca(OH)(CO_3H)\cdot CH_3SO_3H_{(ad)} \quad (2)$$

$$Ca(OH)(CO_3H)\cdot CH_3SO_3H_{(ad)} \rightarrow Ca(OH)(CH_3SO_3)_{(ad)} + H_2CO_{3(ad)} \quad (3)$$

$$H_2CO_{3(ad)} \rightarrow H_2O_{(ad)} + CO_{2(g)} \quad (4)$$

To verify the proposed mechanism, the dependence of reaction rates/uptake coefficients on gaseous MSA concentration, relative humidity, and temperature should be further investigated.

3.4 Uptake coefficients

The uptake coefficient of heterogeneous reactions, γ, is defined as the ratio of the number of gas molecules which reacted with the surface to the number of gas molecules which collided with the surface [27]. The uptake coefficient of the reaction of gaseous MSA with $CaCO_3$ and kaolinite particles was calculated as follows:

$$\gamma = \frac{d[MS^-]/dt}{C} = \frac{d[MS^-]/dt}{A[MSA_{(g)}]v}$$

where $d[MS^-]/dt$ is the production rate of MS^-, C is the collision frequency of gaseous MSA molecules with the surface of the particles, A is the surface area available for the reaction (here the BET surface area of particles was used), $[MSA_{(g)}]$ is the concentration of gaseous MSA, and v is the mean molecule speed of gaseous MSA.

The uptake coefficients (240 min averaged) of the reactions of gaseous MSA with $CaCO_3$ and kaolinite particles at two different gaseous MSA concentrations are shown in Figure 5, where the steady-state uptake coefficients of the reaction of gaseous MSA with NaCl and sea salt particles measured in our previous study [22] are also included for comparison. When the concentration of gaseous MSA was 1.34×10^{13} molecules/cm^3, the uptake coefficient of gaseous MSA was $(1.21\pm0.06)\times10^{-8}$ for the reaction with $CaCO_3$ and

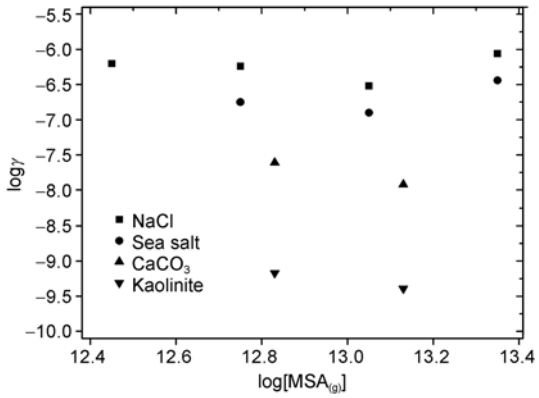

Figure 5 Uptake coefficients of heterogeneous reactions of gaseous MSA with different particles, as a function of gaseous MSA concentration.

was $(4.10\pm0.65)\times10^{-10}$ for the reaction with kaolinite; when the gaseous MSA concentration was 6.72×10^{12} mol/cm^3, the uptake coefficient was $(2.48\pm0.41)\times10^{-8}$ for $CaCO_3$ and $(6.74\pm1.09)\times10^{-10}$ for kaolinite. The uptake coefficients of both reactions decreased with increasing gaseous MSA concentrations, while our previous study suggested that the heterogeneous reactions of gaseous MSA with NaCl and sea salt particles was of first order with respect to MSA. To confirm the reaction orders for gaseous MSA in the reactions with $CaCO_3$ and kaolinite, uptake coefficients should be measured at more gaseous MSA concentrations.

As shown in Figure 5, at similar/same gaseous MSA concentrations, the uptake coefficients for the heterogeneous reaction with NaCl and sea salt were significantly larger than that for $CaCO_3$, which was again much larger than that for kaolinite. The differences in measured uptake coefficients could be at least partially attributable to the different surface characteristics of NaCl, sea salt, $CaCO_3$, and kaolinite. Furthermore, the smaller uptake coefficients for $CaCO_3$ and kaolinite might also be partially due to the larger BET surface area of $CaCO_3$ (0.8772 m^2/g) and kaolinite (24.1059 m^2/g) than that of NaCl and sea salt. Only some parts of the particles' surface could participate in heterogeneous reactions with gaseous MSA, leading to overestimation of the surface area available for the reaction and then underestimation of the uptake coefficients; the deviation might be much more significant for kaolinite because of its much larger BET surface area. If the geometric area, i.e. the cross section of the sample cup, was used to calculate the gas-surface collision frequency, the uptake coefficient of $CaCO_3$ is close to that of kaolinite, though still about one order of magnitude smaller than these of NaCl and sea salt particles.

The uptake coefficients of the reactions of $CaCO_3$ and kaolinite with gaseous MSA were significantly smaller than the corresponding values for the reactions of NaCl and sea salt, and our previous study suggested that the uptake coefficients of the heterogeneous reactions of NaCl and sea salt with gaseous MSA were too low to explain the observed MS^- in the aerosols of the marine boundary layer [22];

therefore, the heterogeneous uptake of gaseous MSA on mineral dust probably does not play an important role in the formation of MS^- in aerosols, although no observation of gaseous MSA in inland boundary layers has been reported. Uptake coefficients at different relative humidity should be determined to further understand the role of the reaction of gaseous MSA with mineral dust in the atmosphere.

4 Conclusions

Heterogeneous reactions of gaseous MSA with $CaCO_3$ and kaolinite particles at room temperature were investigated via DRIFTS and IC, and MS^- was found to be formed on the particles in both reactions. A mechanism for the reaction of gaseous MSA with $CaCO_3$ was proposed, and for the first time the uptake coefficients of the two reactions were determined, which are significantly smaller than those of the corresponding reactions with NaCl and sea salt. To further elucidate the reaction mechanism and to evaluate the role of these reactions in the formation of MS^- in the aerosol, more study is required to study the influence of temperature, relative humidity, and gaseous MSA concentration on the reaction rate, and to solve the problem of underestimation of uptake coefficients by using the BET surface.

This work was supported by National Natural Science Foundation of China (40490265 & 20077001), National Basic Research Program of China (2002CB410802), and special fund of State Key Joint Laboratory of Environment Simulation and Pollution Control.

1 Charlson RJ, Lovelock JE, Andreae MO, Warren SG. Oceanic phytoplankton, atmospheric sulfur, cloud albedo and climate. *Nature*, 1987, 326(16): 655–661
2 Barnes I, Hjorth J, Mihalopoulos N. Dimethyl sulfide and dimethyl sulfoxide and their oxidation in the atmosphere. *Chem Rev*, 2006, 106(3): 940–975
3 Davis D, Chen G, Kasibhatla P, Jefferson A, Tanner D, Eisele F, Lenschow D, Neff W, Berresheim H. DMS oxidation in Antarctic marine boundary layer: Comparison of model simulations and field observations of DMS, DMSO, $DMSO_2$, H_2SO_4(g), MSA(g), and MSA(p). *J Geophys Res-Atmos*, 1998, 103(D1): 1657–1678
4 Davis D, Chen G, Bandy A, Thronton D, Eisele F, Mauldin L, Tanner D, Lenschow D, Fuelberg H, Herbert B, Heath J, Clarke A, Blake D. Dimethyl sulfide oxidation in the equatorial pacific: Comparison of model simulations and field observations of DMS, SO_2, H_2SO_4(g), MSA(g), MS, and NSS, *J Geophys Res-Atmos*, 1999, 104(D5): 5765–5784
5 Bardouki H, Berresheim F, Vrekoussis M, Sciare J, Kouvarakis G, Oikonomou K, Schneider J, Mihalopoulos N. Gaseous (DMS, MSA, SO_2, H_2SO_4, and DMSO) and particulate (sulfate and methanesulfonate) sulfur species over the northeastern coast of Crete. *Atmos Chem Phys*, 2003, 3(5): 1871–1886
6 Andreae MO, Andreae TW. The cycle of biogenic sulfur-compounds over the Amazon basin .1. Dry season. J *Geophys Res-Atmos*, 1988, 93(D2): 1487–1497
7 Yang Z, Kong L, Zhang J, Wang L, Xi S. Emission of biogenic sulfur gases from Chinese rice paddies. *Sci Total Environ*. 1998, 224(1-3): 1–8
8 Yuan H, Wang Y, Zhuang GS. MSA in Beijing aerosol. *Chinese Sci Bull*, 2004, 49(10): 1020–1025
9 Wang Y, Zhuang GS, Tang A H, Yuan H, Sun Y, Chen S, Zheng AH. The ion chemistry and the source of PM2.5 aerosol in Beijing. *Atmos Environ*, 2005, 39(21): 3771–3784
10 Tegen I, Harrison SP, Kohfeld K, Prentice IC, Coe M, Heimann M. Impact of vegetation and preferential source areas on global dust aerosol: Results from a model study. *J Geophys Res*, 2002, 107(D21): DOI: 10.1029/2001JD000963
11 Lunt DJ, Valdes PJ. The modern dust cycle: Comparison of model results with observations and study of sensitivities, *J Geophys Res*, 2002, 107(D23), 4669, doi:10.1029/2002JD002316
12 Luo C, Mahowald NM, del Corral J. Sensitivity study of meteorological parameters on mineral aerosol mobilization, transport, and distribution. *J Geophys Res*, 2003, 108(D15), 4447, doi: 2003JD003483
13 Seinfeld JH, Pandis SN. *Atmospheric Chemistry and Physics: From Air Pollution to Climate Change*. New York: John Wiley and Sons, 1998
14 Duce RA, Unni CK, Ray BJ, Prospero J M, Merrill JTS. Long-range atmospheric transport of soil dust from Asia to the tropical North Pacific-Temporal variability. *Science*, 1980, 209(4464): 1522–1524
15 Baker AR, Kelly SD, Biswas KF, Witt M, Jickells TD. Atmospheric deposition of nutrients to the Atlantic Ocean. *Geophys Res Lett*, 2003, 30(24): doi:10.1029/2003GL018518
16 Mahowald NM, Baker AR, Bergametti G, Brooks N, Duce RA, Jickells TD, Kubilay N, Prospero JM, Tegen I. Atmospheric global dust cycle and iron inputs to the ocean. *Glob Biogeochem Cycle*, 2005, 19(4): doi:10.1029/2004GB002402
17 Dentener FJ, Crutzen PJ. Reaction of N_2O_5 on tropospheric aerosols-impact on the global distributions of NO_x, O_3, and OH. *J Geophys Res-Atmos*, 1993, 98(D4): 7149–7163
18 Dentener FJ, Carmichael GR, Zhang Y, Lelieveld J, Crutzen PJ. Role of mineral aerosol as a reactive surface in the global tropo-sphere. *J Geophys Res-Atmos*, 1996, 101(D17): 22869–22889
19 De Bruyn WJ, Shorter JA, Davidovits P, Worsnop DR, Zahniser MS, Kolb CE. Uptake of gas phase sulfur species methanesulfo-nic acid, dimethylsulfoxide, and dimethyl sulfone by aqueous surfaces. *J Geophys Res-Atmos*, 1994, 16(D8): 16927–16932
20 Schweitzer F, Magi L, Mirabel P, George C. Uptake rate measurement of methanesulfonic acid and glyoxal by aqueous droplet. *J Phys Chem A*, 1998, 102(3): 593–600
21 Hanson DR. Mass accommodation of H_2SO_4 and CH_3SO_3H on water–sulfuric acid solutions from 6% to 97% RH. *J Phys Chem A*, 2005, 109(31): 6919–6927
22 Tang MJ, Zhu T. Heterogeneous reactions of gaseous methanesulfonic acid with NaCl and sea salt particles. *Sci China Ser B-Chem*, 2009, 52(1): 1–8
23 Weaver CE, Pollard LD. *The Chemistry of clay minerals*: London: Elsevier Scientific Publishing Company, 1973
24 Vogt R, Finlayson-Pitts BJ. A diffuse reflectance infrared Fourier transform spectroscopic (DRIFTS) study of the surface reaction of NaCl with gaseous NO_2 and HNO_3, *J Phys Chem*, 1994, 98(14), 3747–3755
25 Li HJ, Zhu T, Ding J, Chen Q, Xu BY. Heterogeneous reaction of NO_2 on the surface of NaCl particles. *Sci China Ser B-Chem*, 2006, 49(4): 371–378
26 Al-Hosney HA, Grassian VH. Carbonic acid: An important intermediate in the surface chemistry of calcium carbonate. *J Am Chem Soc*, 2004, 126(26): 8068–8069
27 Ravishankara AR. Heterogeneous and multiphase chemistry in the troposphere. *Science*, 1997, 276(5315):1058–1065